

Lasers in Manufacturing Conference 2015

# Investigation of the influence of laser surface modifications on the adhesive wear behavior in dry cold extrusion of aluminum

Ingo Roß<sup>a,\*</sup>, André Temmler<sup>b</sup>, Edgar Willenborg<sup>a</sup>,  
Reinhart Poprawe<sup>a,b</sup>, Marco Teller<sup>c</sup>

<sup>a</sup>Fraunhofer Institute for Laser Technology ILT, Steinbachstr. 15, 52072 Aachen, Germany

<sup>b</sup>Chair for Laser Technology LLT, RWTH Aachen University, Steinbachstr. 15, 52072 Aachen, Germany

<sup>c</sup>Institute of Metal Forming IBF, RWTH Aachen University, Intzestr. 10, 52056 Aachen, Germany

---

## Abstract

One of the main wear mechanisms in cold extrusion of aluminum is adhesion. While this can be prevented by excessive usage of lubrication, due to environmental and economic reasons a surface modification which allows dry metal forming, i.e. processing without lubrication is highly desired. In this paper first results concerning the effect of the spectral surface roughness characteristics of laser polished specimens made from AISI D2 cold work steel on their tendency to adhesive wear with aluminum are presented. By using macro polishing as well as micro polishing different spatial wavelength ranges of the surface roughness are modified, resulting in surfaces with a unique spectral roughness distribution. The laser polished specimens are tested in a compression-torsion tribometer under conditions adapted from cold extrusion. Before and after testing the topography of each specimen is measured via white light interferometry. By comparing both topographies the volume of adherent aluminum is determined. The influence of the laser surface modification is investigated on basis of the spectral roughness distribution and the characterization of the adhesive wear behavior.

*Keywords:* laser polishing; adhesion; wear; cold extrusion; compression-torsion tribometer

---

---

\* Corresponding author. Tel.: +49-241-8906-8196; fax: +49-241-8906-121.  
E-mail address: ingo.ross@ilt.fraunhofer.de.

## 1. Introduction

Tools for cold extrusion are subject to contact stresses of up to 6.4 times the initial yield stress of the workpiece material [Geiger et al., 2012], making the excessive lubrication a key factor in enhancing a tool's endurance as well as in reducing the necessary process forces. Depending on the combination of tool and workpiece material, different kinds of lubricants such as oils, alkaline or zinc soaps are commonly used [Bay, 1994]. These lubricants usually have to be removed before further processing. The thus needed cleaning steps are often time-consuming and involve chemical agents that are potentially harmful for the environment. Therefore, a surface modification, which allows processing without additional lubrication is highly desirable. This kind of dry metal forming is defined by Vollertsen and Schmidt as "a process where a workpiece leaves the forming tool without the necessity of cleaning or drying before further production steps" [Vollertsen and Schmidt, 2014].

In this paper first results concerning the influence of the spectral surface roughness characteristics of laser polished specimens made from AISI D2 cold work steel (X153CrMoV12) on their tendency to adhesive wear with pure aluminum (AA1050-O) under dry metal forming conditions are presented. The wear tests are performed on a compression-torsion tribometer under testing conditions which correspond to the load spectrum of cold forward rod extrusion. By using macro polishing with continuous wave as well as micro polishing with pulsed laser radiation different spatial wavelength ranges of the surface roughness are modified, resulting in surfaces with a unique spectral roughness distribution. Specimens with a ground surface serve as reference. Optical measurements of the contact surface before and after testing are used for the evaluation of the adhering material.

## 2. Process fundamentals of laser polishing

Laser polishing of metallic surfaces is based upon a micro remelting process, optimized for smoothing the initial topography: A thin layer is molten by laser radiation and surface structures are reduced in the molten state by the surface tension in the melt pool. In contrast to conventional grinding and polishing processes the material is not removed, but only redistributed. Areal polishing is achieved by scanning the laser spot in a meander pattern over the workpiece surface. Fig. 1 shows the schematic of the laser polishing process and the main process parameters, which are to be chosen depending on the material, the initial roughness and the target roughness. [Willenborg, 2006]

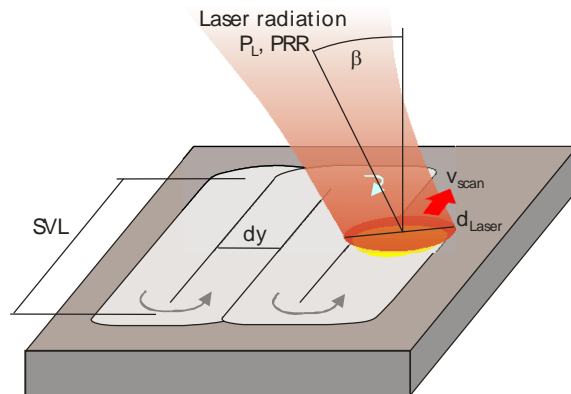


Fig. 1. Schematic of the laser polishing process with the main process parameters: laser power  $P_L$ , pulse repetition rate  $PRR$ , laser spot diameter  $d_{Laser}$ , scan velocity  $v_{scan}$ , track offset  $dy$ , scan vector length  $SVL$ , angle of incidence  $\beta$ . [Willenborg, 2006]

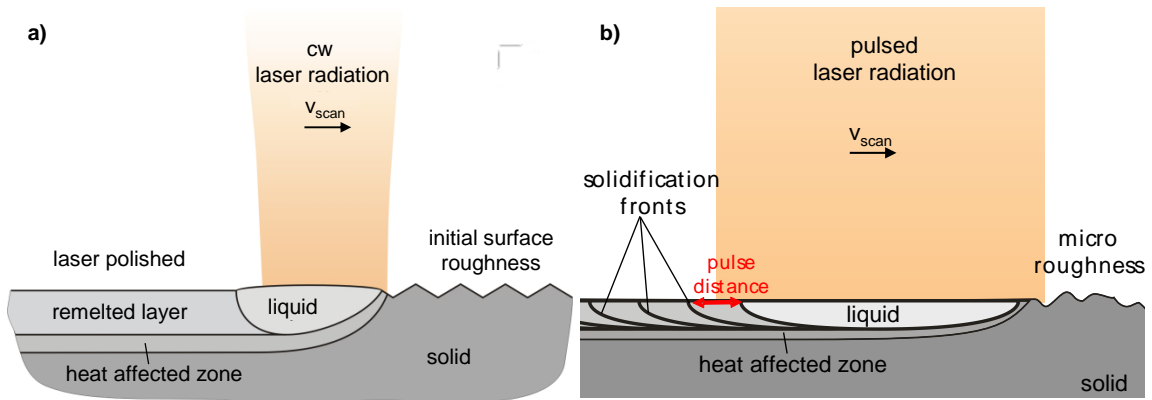


Fig. 2. Process principle of the laser polishing process: a) macro laser polishing with continuous wave laser radiation; b) micro laser polishing with pulsed laser radiation. [Willenborg, 2006]

For laser polishing of metals there are two process variants: macro polishing, using continuous wave (cw) laser radiation (Fig. 2a) and micro polishing with pulsed laser radiation (Fig. 2b). Typical melting depths for macro polishing range from 20-100  $\mu\text{m}$  allowing the smoothing of coarse surface structures such as milling and turning tracks or grinding marks, whereas the micro polishing process leads to melting depths of less than 5  $\mu\text{m}$  [Bordatchev et al., 2014; Nüsser et al., 2015]. Consequently, micro polishing enhances the micro roughness and glossiness while leaving bigger structures untouched [Temmler, 2013]. The initial roughness of a workpiece can be Ra 1.0  $\mu\text{m}$  or higher for macro polishing and should typically be less than Ra 0.8  $\mu\text{m}$  for micro polishing.

### 3. Set-up

#### 3.1. Laser polishing machine

The experiments were performed on a laser polishing machine developed by the Fraunhofer-Institute for Laser Technology (ILT), Aachen, Germany. This machine uses 5 mechanical axes (three linear and two rotatory) for aligning the workpiece relative to the optical system, while a 3-axis galvanometer mirror system by Scanlab deflects the focused laser beam three-dimensionally onto the workpiece surface. The laser beam is focused by an f-theta scan lens and the laser spot diameter can be continuously changed from  $d_L = 125\text{-}800 \mu\text{m}$  using a motorized zoom telescope. The laser source used in this investigations is a fiber-coupled Q-switch Nd:YAG solid-state laser ( $\lambda_{em} = 1064 \text{ nm}$ ;  $P_{L,max} = 400 \text{ W}$ ). In order to reduce oxidation, the workpiece is placed in a process chamber with inert gas during laser polishing. The residual oxygen is controlled by a closed-loop control.

#### 3.2. Compression-Torsion Tribometer

The wear experiments are performed on a compression-torsion tribometer as described in [Teller et al., 2015a; Teller et al., 2015b]. In this tribometer, the tool specimen (Fig. 3), loaded axially by a pneumatic cylinder, is pressed onto the rotating workpiece specimen. A test cycle consists of the following phases:

- Workpiece specimen rotates at a constant velocity;
- Tool specimen is pressed onto the workpiece specimen until a preset load is reached;

- Relative movement and load are maintained for a particular number of revolutions;
- Tool specimen is unloaded;
- Rotation of workpiece specimen stops after separation.

The compression-torsion tribometer can use rotation velocities of up to 80 rpm and loads of up to 18kN. The contact pressure can be scaled to a multiple of the initial yield stress of the workpiece material by an encapsulation of the workpiece specimen (Fig. 3). During testing, the torque transferred from the rotated to the stationary side, the load and the glide length are measured.

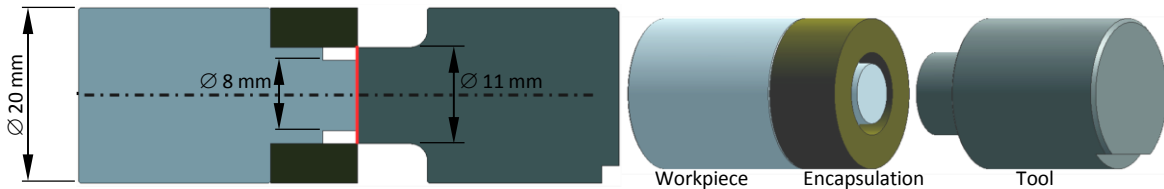


Fig. 3. Schematic of the test specimen for the compression-torsion tribometer. [Teller et al., 2015a]

### 3.3. Surface characterization

For the evaluation of a surface's quality, profile or areal roughness parameters such as Ra, Rq, Rz respectively Sa, Sq, Sz are widely used. Although these parameters are sufficient for the comparison of surfaces with similar characteristic, the limits become evident when comparing surfaces which were processed with different technologies, e. g. milled, ground and laser polished surfaces. All of these might show the same areal roughness Sa, but can be distinguished visibly by their respective structural characteristics. By analyzing the surfaces in regard of the predominance of structures with specific spatial wavelengths, i.e. a spectral roughness analysis, a more detailed comparison and evaluation of experimental results is possible. For this, the surface topography of a workpiece is measured optically by white light interferometry. The data is then analyzed using phase-correct band pass filters, thus allowing the calculation of the areal roughness for discrete ranges of spatial wavelength of the different surface structures [Temmler, 2013]. Fig. 4 gives an overview of this method: The measurements are performed at various magnifications, each of which is used for the analysis of a different set of spatial wavelengths, and the results are plotted as a roughness spectrum, reflecting the surfaces characteristics. E.g. the roughness spectrums of milled or turned surfaces will typically show a local maximum at the spatial wavelength that represents the used track offset.

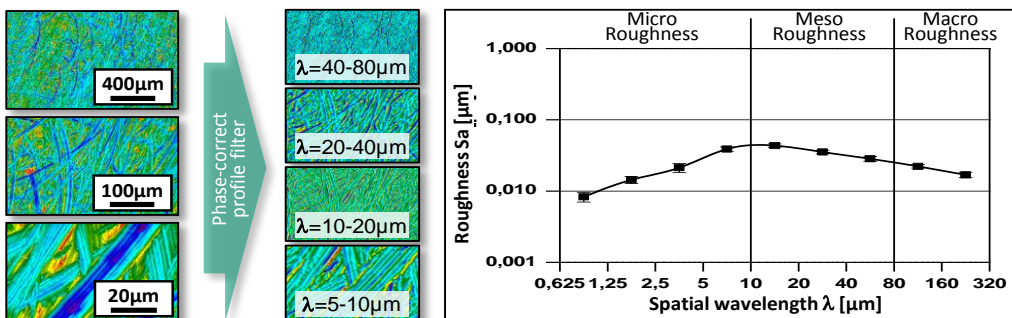


Fig. 4. Schematic of the roughness spectrum analysis with white light interferometry surface measurements at different magnifications.

## 4. Experimental

For this investigation, laser polishing tests with cw and pulsed laser radiation are performed on 110x120x25 mm<sup>3</sup> AISI D2 cold work steel slabs. The initial surface is ground to a roughness of  $R_a = 0,49 \pm 0,02 \mu\text{m}$ . The laser spot diameter  $d_L$ , the track offset  $dy$  and the residual oxygen  $c_{O_2}$  in the shielding atmosphere are constant. The test field size is 10x10 mm<sup>2</sup>. Table 1 shows a summary of the tested laser parameters. All laser polished surfaces are analyzed using the roughness spectrum as described in chapter 3.3. Additionally the roughness of macro laser polished surfaces is measured using a Mahr M2 tactile profilometer. Based on the results on the slabs, tribometer specimens are polished with three different parameter sets for the wear test. Additionally, specimens with the initial surface are tested as a reference. All tool specimens were heat treated under vacuum, resulting in a hardness of 58-62 HRC. The tool specimens have a contact area of  $A_{tool} = 95.03 \text{ mm}^2$ . The workpiece material is pure aluminum in an annealed state (AA1050-O; initial yield stress  $\sigma_{y0} = 25 \text{ MPa}$ ). The testing conditions are adopted from cold forward rod extrusion. The axial loading is selected to 14.5 kN, leading to a relative surface pressure (contact stress  $p$  divided by the initial yield stress  $\sigma_{y0}$ ) of approximately six. The experiments are performed with a rotation speed of 60 rpm and a glide distance of two revolutions at full load. Experiments are conducted in dry state.

Table 1. Summary of investigated laser polishing parameters

Laser polishing parameters	
Laser spot diameter $d_L$	250 $\mu\text{m}$
Laser power $P_L$	30-160 W
Pulse repetition rate $PRR$	cw /20kHz
Scan velocity $v_{scan}$	100 mm/s (cw) 1000 mm/s (pulsed)
Track offset $dy$	30 $\mu\text{m}$
Number of passes $n$	1-4
Shielding gas	Argon
Residual oxygen $c_{O_2}$	1000 ppm

In order to characterize the adhesive wear behavior the test surface of each specimen is fully measured using the Zygo NewView7300 white light interferometer before and after testing on the tribometer. The initial topography is subtracted from the worn topography after testing. The difference of these data sets represents the adherent material, which is analyzed in regard to quantity and distribution. For the analysis in chapter 5.3 a threshold of  $h_{adhesion, min} = 0.1 \mu\text{m}$  is defined. Detected data points with a smaller height are ignored in the calculation of the overall volume of adherent material. Consequentially, an uncertainty of approx.  $5 \times 10^{-3} \text{ mm}^3$  has to be taken into account, presuming an areal adhesion of up to 50% of the contact surface with a height of 0.1 mm

## 5. Results and discussion

### 5.1. Laser polishing

The theoretical limits of the process window for the laser polishing process are set by its definition as a remelting process: The amount of energy that is necessary to melt the material marks the lower limit, while the upper limit is set by the threshold, where the material starts to evaporate. Additionally, the applied energy has to be sufficient for melting the initial surface structures and chosen in such a way that new surface structures induced by the process do not increase the initial roughness [Nüsser et al., 2015]. The variation of the laser power and number of passes for the macro (cw) laser polishing process with constant laser spot diameter  $d_L$  and scan velocity  $v_{scan}$  is shown in Fig. 5a. Compared to the initial surface the roughness is slightly increased at  $P_{L,cw} = 60$  W and  $n = 1$ . With increasing laser power the roughness is decreased to a local minimum. Higher laser powers then lead to a relative increase of the surface roughness. Tests with more than 1 pass show a further decrease of the surface roughness. At  $P_{L,cw} = 120$  W and  $n = 4$  a roughness  $Ra_{tactile} = 0.20 \pm 0,02 \mu\text{m}$  is achieved. The comparison of the roughness spectrum of the best three parameters is shown in Fig. 5b. All three spectrums show a reduced roughness for spatial wavelengths  $\lambda$  between 2.5-320  $\mu\text{m}$ . In the micro roughness range of  $\lambda < 40 \mu\text{m}$  the 120 W test field has the smallest roughness, while the 100 W test field leads to a smaller roughness for spatial wavelengths of  $\lambda > 40 \mu\text{m}$ . Due to the small tactile roughness and the improved micro roughness, the parameters  $P_{L,cw} = 120$  W,  $n = 4$  are used in the following investigations.

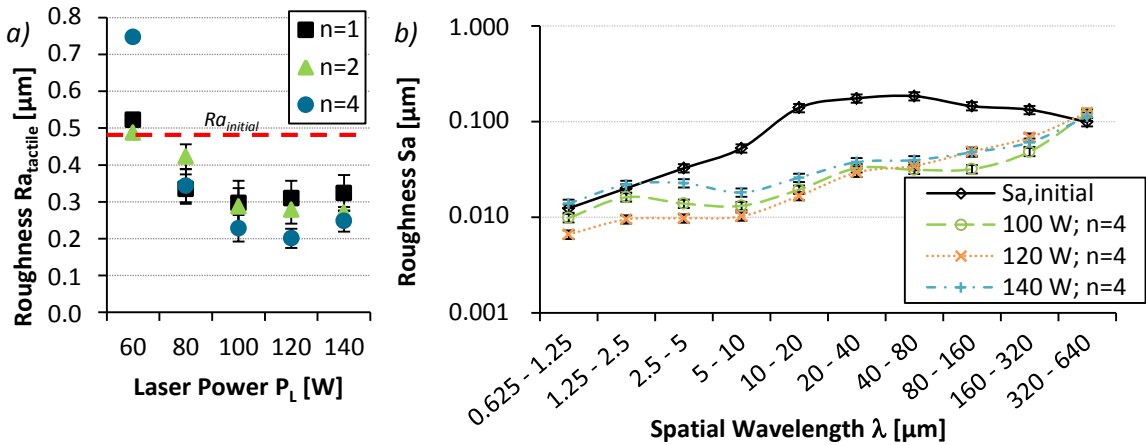


Fig. 5: Tactile roughness after macro (cw) laser polishing with 1-4 passes (a) and roughness spectrum after macro (cw) laser polishing with 4 passes (b).

As was mentioned above, micro laser polishing can improve the micro roughness while leaving bigger structures untouched. Thus, a combination of macro and micro laser polishing was investigated. Fig. 6 shows the results for the laser power variation for the micro polishing process. All micro polishing tests are performed with  $n = 1$ . Before micro polishing, all test fields were macro polished with the determined reference parameters. At a laser power of  $P_{L,pulsed} = 30$  W, the micro roughness for  $\lambda < 10 \mu\text{m}$  is reduced as compared to the macro polished surface without affecting the rest of the spectrum. At 50 W the micro roughness for  $\lambda < 5 \mu\text{m}$  is further decreased, while an increase can be detected for  $\lambda = 5-20 \mu\text{m}$ . Higher laser powers further increase the roughness compared to the 50 W parameter. The increase in the wavelength

range of 20-40  $\mu\text{m}$  at high laser power can be attributed to border bulging of the melt pool due to increased vapour pressure [Nüsser et al., 2015] and the track offset of  $dy = 30 \mu\text{m}$ .

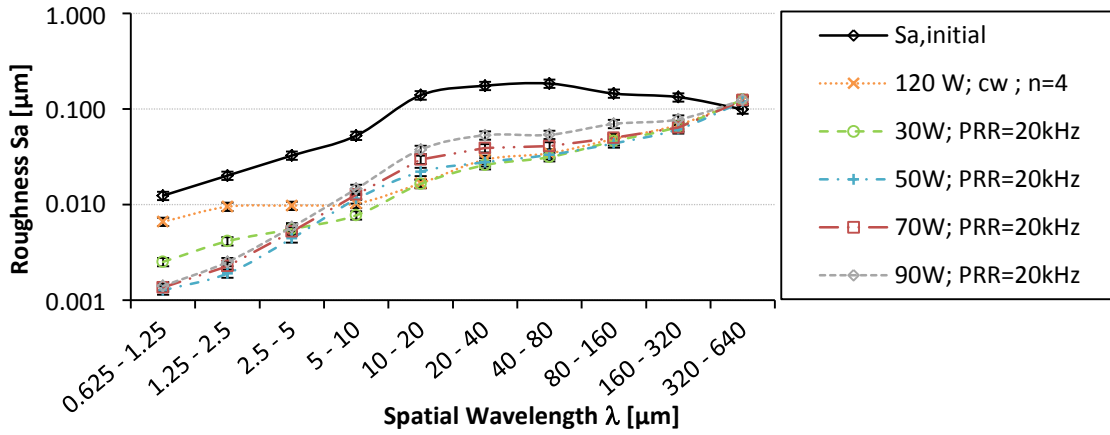


Fig. 6. Roughness spectrum after combined macro (cw) and micro (pulsed) laser polishing: variation of laser power for micro polishing; cw parameters constant ( $P_{L,cw} = 120 \text{ W}$  and  $n = 4$ ).

In order to evaluate the influence of the surface remelting during macro polishing on the micro polishing process, the same parameters as in the investigation of the macro/micro polishing combination were used on the initial surface. The comparison of the initial surface and the macro, micro and macro/micro polished surfaces can be seen in Fig. 7. With macro polishing the initial ghost lines are fully remelted (b), while remains of the grinding structure can still be seen after micro polishing (c). Neither ghost lines nor the laser polishing tracks can be seen after the combination of micro and macro polishing (d).

Based on the roughness results, the parameter sets for macro ( $P_{L,cw} = 120 \text{ W}$ ,  $n = 4$ ), micro ( $P_{L,pulsed} = 50 \text{ W}$ ) and combined macro/micro polishing are chosen for testing on the tribometer.

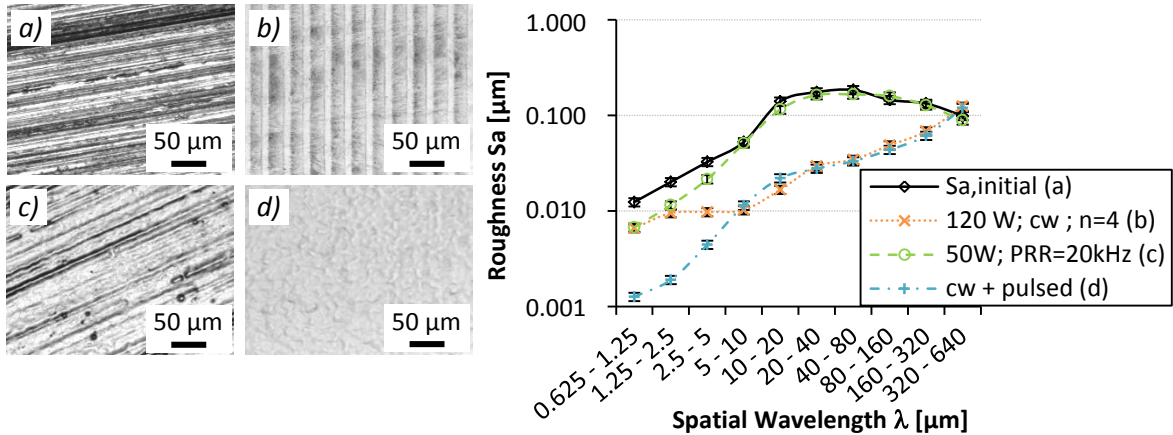


Fig. 7. Summary of the chosen surfaces for testing on the tribometer: a) initial surface; b) macro polished; c) micro polished; d) macro/micro polished.

### 5.2. Tribometer specimens

For each of the chosen parameter sets two tribometer specimens are laser polished. While the micro polishing result on the tribometer specimens is as to be expected from the test on slab material, the results for macro and macro/micro polishing show a deviation from the above presented investigations. The spectrums in Fig. 8 show that for spatial wavelengths smaller than  $80\ \mu\text{m}$  the tribometer specimens' roughness is significantly higher than the results on slab material. Furthermore, the tribometer specimens show annealing colors after laser polishing which do not occur on slab material when using the same parameters. The reason for this deviation might be attributed to a difference in the heat conduction boundaries: The big slab material presumably allows the conduction of significantly more energy than the smaller tribometer specimens thus leading to a difference in substrate temperature during laser polishing. However, the influence of the micro polishing step on the micro roughness of a beforehand macro polished surface is qualitatively the same for both the tribometer specimens and the slab material.

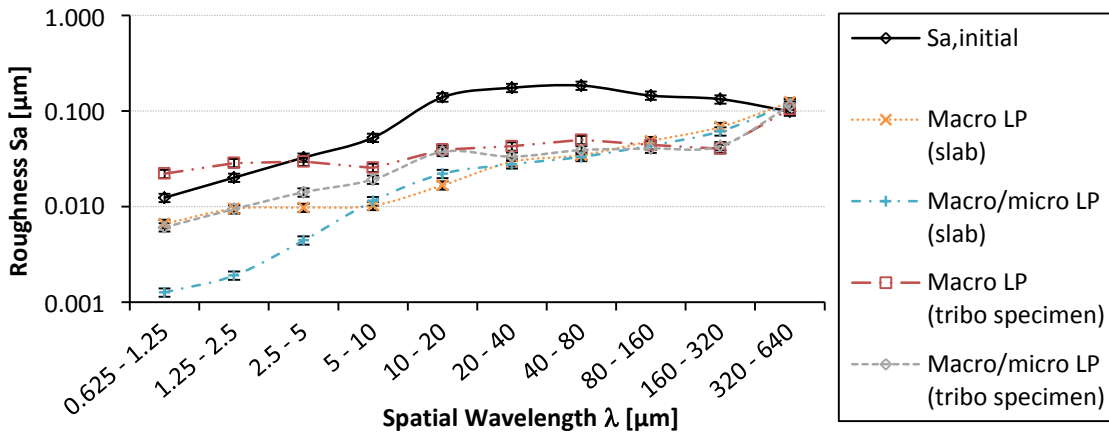


Fig. 8. Roughness spectrum comparison of laser polished slab and tribometer test specimens: macro LP (laser polishing) parameters:  $P_{L,cw} = 120\ \text{W}$ ,  $n = 4$ ; macro/micro LP parameters:  $P_{L,cw} = 120\ \text{W}$ ,  $n = 4 + P_{L,pulsed} = 50\ \text{W}$ .

### 5.3. Wear characterization

The analysis of the adherent material after the tribometer test shows the influence of the surface modification by laser polishing on the wear characteristic (Fig. 9). The graph shows the distribution of adherent material depending on the radial position. The surface is divided in ring segments of the same size. For each ring segment the corresponding volume, normalized to the ring segment's surface area, is plotted. On the specimens with the ground initial surface (a) several big adhesions can be found both in the middle area and at the outer radius. Smaller amounts of aluminum preferably stick alongside of ghost lines of the initial surface. This hints at a combination of abrasive and adhesive wear mechanisms. The macro polished specimens (b) do not have any ghost lines. Consequentially, the adherent material is only oriented circularly, following the relative movement of the rotating specimen during the wear test. Although, the wear characteristics for these two surfaces differ from each other, their overall volume of adherent aluminum is similarly big: approx.  $50\text{-}200 \times 10^{-3}\ \text{mm}^3$  for the initial surface and approx.  $120\text{-}160 \times 10^{-3}\ \text{mm}^3$  for the macro polished surface. The micro polished specimen (c) shows slightly less adhesive wear in the inner area of the contact surface (Fig. 9 right; radius up to  $5\ \text{mm}$ ) than the former specimens. The overall volume of adherent



material is approx.  $40\text{-}85 \times 10^{-3} \text{ mm}^3$ . The smallest amount of adhesive wear is detected for the specimens that are macro and micro polished (d): both tested specimens show an overall adhesion volume of approx.  $5.5 \times 10^{-3} \text{ mm}^3$ .

Considering the wear test results, a closer examination of the roughness spectrums suggests that, for the investigated tool/workpiece material combination, a reduced micro roughness for  $\lambda < 5 \mu\text{m}$  (c; Fig. 7) is beneficial for the wear behavior as compared to the ground surface (a). In contrast, the reduced meso and macro roughness for  $\lambda = 5\text{-}320 \mu\text{m}$  and increased micro roughness for  $\lambda < 5 \mu\text{m}$  of the macro polished specimen does not reduce the amount of adherent aluminum, but possibly shifts the balance between the abrasive and adhesive wear mechanisms, thus leading to the observed change in the wear characteristic. In addition to the roughness spectrum, the surface oxidation (see chapter 5.2) of the macro and combined macro/micro polished specimens might have an influence on the wear behavior that has to be taken into account in future investigations.

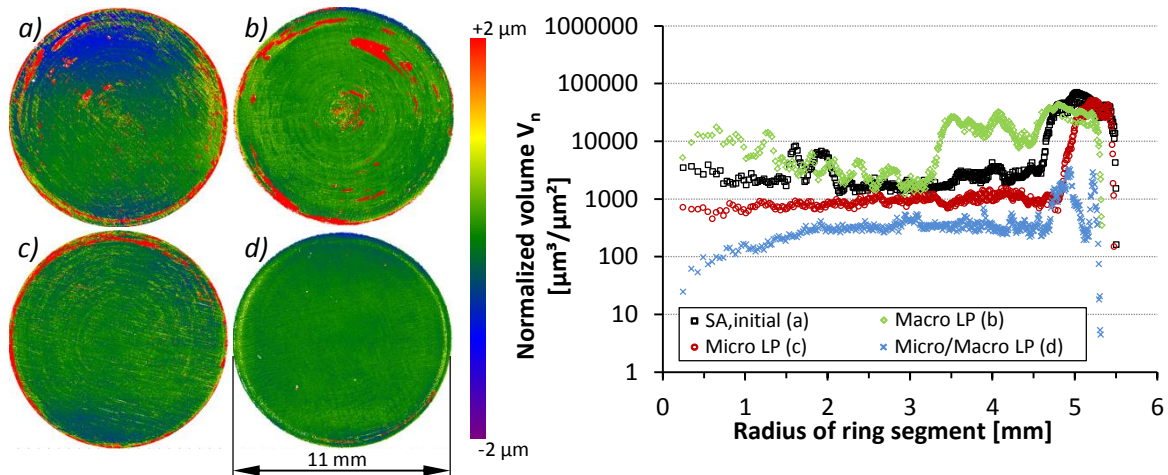


Fig. 9. Adherent material on exemplary tribometer specimens in false colors (left) and normalized volume distribution of adherent material depending on the radial position (right): a) initial surface; b) macro polished; c) micro polished; d) macro/micro polished.

## 6. Summary and outlook

Laser polishing is a new approach for improving the surface roughness without the removal of any material. Compared to well-established processes like milling, turning, EDM or abrasive polishing, surfaces with completely new roughness characteristics can be created. By specific adjustment of the laser parameters different parts of a surface's spectral roughness can be influenced. In this investigation parameters for both macro and micro laser polishing AISI D2 cold work steel were developed. With the former a roughness of down to  $Ra_{\text{tactile}} = 0.20 \pm 0.02 \mu\text{m}$  was achieved on ground test specimens, while with the latter the micro roughness for  $\lambda < 5 \mu\text{m}$  was enhanced.

Furthermore, first results concerning the influence of laser polishing on the wear behavior were presented. Three different laser polished surfaces were tested on a compression-torsion tribometer and compared to specimens with the initial surface. Each of the laser polishing parameter sets lead to a different change in the adhesive wear behavior of the tribometer specimens compared to the initial surface. By using

a combined macro/micro laser polishing process, the overall volume of adherent material was reduced by a factor of approx. 10 as compared to the ground surface.

The investigation of the roughness spectrums suggests a correlation of the micro, meso and macro roughness on the balance of the abrasive and adhesive wear mechanisms. However, for a more detailed evaluation of the influence, additional surface types with various roughness spectrums as well as the reproducibility have to be investigated.

Future investigations will thus involve the following topics:

- Reproducibility of the above shown results;
- Development and test of new laser polishing parameters for specifically optimized roughness spectrums;
- Development and test of parameters for surface structuring by remelting, which allows the modification of the long-wave range of the spectral roughness;
- Influence of the annealing state and surface oxidation due to laser polishing on the wear behavior;
- Wear tests with increased glide distances and higher relative velocities.

## Acknowledgements

The authors gratefully acknowledge the financial support of the Deutsche Forschungsgemeinschaft (DFG) within the priority programme SPP 1676 "Dry Metal Forming".

## References

- Geiger, M., Herlan, T., 2012. Fließpressen, in „Handbuch Umformen: Handbuch der Fertigungstechnik“ G. Spur, H. Hoffmann, R. Neugebauer, Editors. Hanser Verlag, München, p. 318.
- Bay, N., 1994. The state of the art in cold forging lubrication, *Journal of Materials Processing Technology* 46, p. 19.
- Vollertsen, F., Schmidt, F., 2014. Dry Metal Forming: Definition, Chances and Challenges, *Int. Journal of Precision Engineering and Manufacturing-Green Technology* 1, p. 59.
- Willenborg, E., 2006. Polieren von Werkzeugstählen mit Laserstrahlung. Dissertation, RWTH Aachen University.
- Bordatchev, E., Hafiz, A., Tutunea-Fatan, O., 2014. Performance of laser polishing in finishing of metallic surfaces, *International Journal of Advanced Manufacturing Technology* 73, p. 35.
- Nüsser, C., Kumstel, J., Kiedrowski, T., Diatlov, A., Willenborg, E., 2015. Process- and Material-Induced Surface Structures During Laser Polishing, *Advanced Engineering Materials* 17, p. 268.
- Temmler, A., 2013. Selektives Laserpolieren von metallischen Funktions- und Designoberflächen. Dissertation, RWTH Aachen University.
- Teller, M., Bambach, M., Hirt, G., Ross, I., Temmler, A., Poprawe, R., Bolvardi, H., Prünke, S., Schneider, J. M., 2015a. Investigation of the suitability of surface treatments for dry cold extrusion by process-oriented tribological testing, *Key Engineering Materials* 651-653, p. 473.
- Teller, M., Bambach, M., Hirt, G., 2015b. A compression-torsion-wear test achieving contact pressures of up to eight times the initial flow stress of soft aluminium, *CIRP Annals* 64, Vol. 1, in press.